J. Cent. South Univ. (2015) 22: 3079−3086
DOI: 10.1007/s11771-015-2844-8

Springer

Energy analysis of face stability of deep rock tunnels using nonlinear Hoek-Brown failure criterion

ZHANG Jia-hua(张佳华), LI Yong-xin (李永鑫), XU Jing-shu (许敬叔)

School of Civil Engineering, Central South University, Changsha 410075, China

Abstract: The nonlinear Hoek-Brown failure criterion was introduced to limit analysis by applying the tangent method. Based on the failure mechanism of double-logarithmic spiral curves on the face of deep rock tunnels, the analytical solutions of collapse pressure were derived through utilizing the virtual power principle in the case of pore water, and the optimal solutions of collapse pressure were obtained by using the optimization programs of mathematical model with regard of a maximum problem. In comparison with existing research with the same parameters, the consistency of change rule shows the validity of the proposed method. Moreover, parametric study indicates that nonlinear Hoek-Brown failure criterion and pore water pressure have great influence on collapse pressure and failure shape of tunnel faces in deep rock masses, particularly when the surrounding rock is too weak or under the condition of great disturbance and abundant ground water, and in this case, supporting measures should be intensified so as to prevent the occurrence of collapse.

Key words: tunnel face; limit analysis; failure criterion; pore water pressure; collapse pressure

1 Introduction

It is frequently to see the collapse of tunnel faces under excavations. Since the original equilibrium of surrounding rock in front of tunnel faces is disturbed with the soil excavations, it induces great deformation until the occurrence of collapse, which not only poses a great threat to the life of construction workers but also leads to unmeasurable loss of the whole project. Therefore, engineers have focused on the research of face stability of tunnels, which has important scientific value and practical significance [1−2].

The issue of face stability in tunnels is certainly a rather tough problem since it is related to many factors, such as the level of surrounding rock, ground water, the size of cross-sections, the way of excavation. The determination of collapse pressure, i.e. calculating the minimal supporting pressure for maintaining the stability of tunnel faces, has become the focus of current investigation [3−5]. According to the limit analysis method, the failure mode of tunnel faces should be established to work out the minimal supporting pressure, while sorely a few scholars have investigated this problem. LECA and DORMIEUX [6] proposed a conical failure mechanism for tunnel faces, and the minimal supporting pressure obtained from limit analysis approach is close to the results of centrifuge tests, which verified the validity of proposed collapse mode. Afterwards, SOUBRA [7] and MOLLON et al [8] constructed a multi-block translational failure mechanism and greatly improved the failure mechanism by which the more optimal results were derived with limit analysis approach since they are more close to the solutions obtained from centrifuge tests. Based on the multi-block translational failure mechanism, limit analysis method and numerical simulation approach were conducted to estimate the stability of tunnels, from which the influence rule of certain parameters on the coefficient of rock weight per volume was gained [9−10]. MOLLON et al [11−12] utilized a spatial discretization technique, i.e. a point-to-point method, to generate the rotational failure mechanism, by which the optimal solutions were also obtained. SUBRIN and WONG [13] constructed a double-logarithmic curved collapse mode according to the failure shape of tunnel faces gained from centrifuge tests, and the calculation results show this suggested failure mode is superior to the multi-block translational failure mechanism.

Consequently, on the basis of the double-logarithmic rotational failure mode, the face stability of deep rock tunnels was investigated under the effect of pore water pressure by utilizing nonlinear Hoek-Brown failure criterion and limit analysis method, which would

Foundation item: Project(2013CB036004) supported by National Basic Research Program of China; Projects(51178468, 51378510) supported by National Natural Science Foundation of China; Project(CX2013B077) supported by Hunan Provincial Innovation Foundation for Postgraduate, China
Received date: 2014−07−07; **Accepted date:** 2014−10−20
Corresponding author: ZHANG Jia-hua, PhD Candidate; Tel: +86−13548600543; E-mail: 124801035@csu.edu.cn

provide theoretical guidance and reference value for supporting design of tunnel faces in deep rock stratum.

2 Definition and theorem

2.1 Nonlinear Hoek-Brown failure criterion

Hoek-Brown failure criterion is an empirical formula of rock failure, which stems from the study of integral brittle rock and the investigation of joint rock mass model. For the sake of application in the practical projects, it has been greatly modified five times, and the current one, i.e. nonlinear Hoek-Brown failure criterion, has been widely utilized in the geotechnical engineering, which can be expressed as [14−18]

$$\sigma_1 = \sigma_3 + \sigma_{ci}\left(m_b\frac{\sigma_3}{\sigma_{ci}} + s\right)^a \tag{1}$$

where σ_1 and σ_3 indicate the maximal and minimal principal effective stresses of rock in failure, respectively; σ_{ci} is the uniaxial compressive strength of rock; m_b, s and a are dimensionless parameters which are related to the characteristics of rock and can be expressed as

$$m_b = m_i \exp\left(\frac{I_{GS}-100}{28-14D}\right) \tag{2}$$

$$s = \exp\left(\frac{I_{GS}-100}{9-3D}\right) \tag{3}$$

$$a = \frac{1}{2} + \frac{1}{6}(e^{-I_{GS}/15} - e^{-20/3}) \tag{4}$$

where I_{GS} is the geological strength index of the rock mass; m_i is the rock constant; D shows the disturbance factor of the rock mass.

Concerning Hoek-Brown nonlinear failure criterion, YANG and YIN [19−20] proposed a tangential technique, shown in Fig. 1. In the stress coordinate system, nonlinear failure criterion is expressed with a curved line, i.e. drawing a tangential line to the curve at the location of tangency point M which presents an angle of φ_t to the direction of σ_n-axis, and the intercept of the straight line, c_t with the τ-axis, thus the expression of the tangential line is

$$\tau = c_t + \sigma_n \tan\varphi_t \tag{5}$$

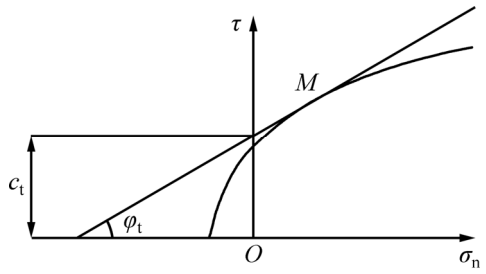

Fig. 1 Tangential line of nonlinear failure criterion

Based on tangential technology, YANG and YIN [21], and MAO et al [22] further studied the nonlinear Hoek-Brown failure criterion and gained the correlation of c_t and φ_t, i.e.

$$\frac{c_t}{\sigma_{ci}} = \frac{\cos\varphi_t}{2}\left[\frac{m_b a(1-\sin\varphi_t)}{2\sin\varphi_t}\right]^{\frac{a}{1-a}} - \frac{\tan\varphi_t}{m_b}\left(1+\frac{\sin\varphi_t}{a}\right)\cdot \left[\frac{m_b a(1-\sin\varphi_t)}{2\sin\varphi_t}\right]^{\frac{1}{1-a}} + \frac{s}{m_b}\tan\varphi_t \tag{6}$$

Applying limit analysis upper bound theorem to compute the research problem, Eq. (6) was adopted to deduce the analytic solutions of supporting pressure of tunnel faces.

2.2 Upper bound theorem under effect of pore water pressure

Pore water pressure has vital impact on the shear strength of rock/soil masses and the stability of geotechnical engineering. In stability problems of geotechnical engineering, pore water pressure is generally drawn by the following two methods [23−24]. It can be obtained simply based on the positions of both ground water drift and saturation line, and it can also be regarded as part of soil gravity, which was put forward by BISHOP in 1955, and the expression can be written as

$$u = r_u \gamma z \tag{7}$$

where u is pore water pressure; r_u is the coefficient of pore water pressure; γ means soil weight per volume; z shows the vertical distance between a random point of soil masses and the ground surface.

Pore water pressure was analyzed as the internal force or the external force in upper bound theorem by some scholars. The results show that the work rate produced both in the region of soil strain and on the boundary by pore water pressure taken as the external force is equivalent to the power of seepage force and buoyancy when it was seen as the internal force, and the equation can be expressed as [25−26]

$$-\int_V u\dot{\varepsilon}_{ij}\mathrm{d}V - \int_S u n_i v_i \mathrm{d}S = -\gamma_w \int_V \frac{\partial h}{\partial x_i} v_i \mathrm{d}V + \gamma_w \int_V \frac{\partial Z}{\partial x_i} v_i \mathrm{d}V \tag{8}$$

where the first integral is the power of producing soil body strain by pore water; the second is the work rate of acting on the boundary by pore water; the third is the power of seepage force; and the last is the work rate of buoyancy. Besides, u is the pore water pressure; $\dot{\varepsilon}_{ij}$ is the body strain; V is the volume; n_i is the outward unit normal vector of failure surface; v_i is the velocity of failure surface; S is the failure surface; γ_w is the unit weight of water; h is the water head; and Z is the

elevation head.

However, it is clearer and easier to accept that pore water pressure is considered the external force. Therefore, pore water pressure was usually taken as the external force to introduce into upper bound theorem for the stability problem of geotechnical engineering, so was this work. As to upper bound theorem of limit analysis, CHEN [27] proposed that the load calculated through equating the external work rate to the internal energy dissipation of rock/soil masses is no less than the actual load in kinematically admissible velocity field. In conclusion, upper bound theorem under the effect of pore water pressure can be written as [28−31]

$$\int_A \sigma_{ij}\dot{\varepsilon}_{ij}\mathrm{d}A \geq \int_S T_i v_i \mathrm{d}S + \int_A F_i v_i \mathrm{d}A + \int_A u_i \dot{\varepsilon}_{ij}\mathrm{d}A + \int_l u_i v_i \mathrm{d}l \tag{9}$$

where the left integration shows the internal energy dissipation created by stress σ_{ij} in the virtual strain field $\dot{\varepsilon}_{ij}$ in the plasticity region A; the right integrations are external work rates which in turn mean the power of external load T_i along the direction of velocity v_i on the boundary S, the work rate of volume force F_i along the direction of v_i in region A, the power of producing soil body strain $\dot{\varepsilon}_{ij}$ in region A and acting on the detaching line l along the direction of velocity v_i by pore water pressure u_i.

According to upper bound theorem, certain assumptions should be introduced as follows. 1) Rock/soil masses should be perfectly plastic material, and it should follow associated flow rule, thus under the nonlinear failure criterion, discontinuous velocity v_i presents an angle of φ_t with the velocity discontinuity line. 2) The sliding block should be regarded as the rigid block which means the volume is a constant in failure. In this case, the virtual strain field is equal to $\dot{\varepsilon}_{ij}=0$ in the region A, and the internal energy dissipates along the velocity detaching line l, thus the power of u_i in the virtual strain field $\dot{\varepsilon}_{ij}$ equates zero.

3 Failure mode

When the tunnel face collapses, the rock/soil masses in front of tunnel face experience heterogeneous velocity field. Based on the double-logarithmic curved failure mechanism proposed by SUBRIN and WONG [13], shown in Fig. 2, the face stability of deep rock tunnels was studied with limit analysis approach. In Fig. 2, AB is the tunnel face with the diameter of d, AE and BE are the two logarithmic spiral lines separately which rotate with a constant angular velocity ω with regard to the center O. Thereinto, the length of OA is r_a and the length of OB is r_b. Meanwhile, among for OB, OA and OE, each has an angle of θ_1, θ_2 and θ_3 with the direction of the vertical line. σ_T indicates the supporting pressure applied on the tunnel face. h characters the height between the underground waterline and the tunnel roof; u is the pore water pressure.

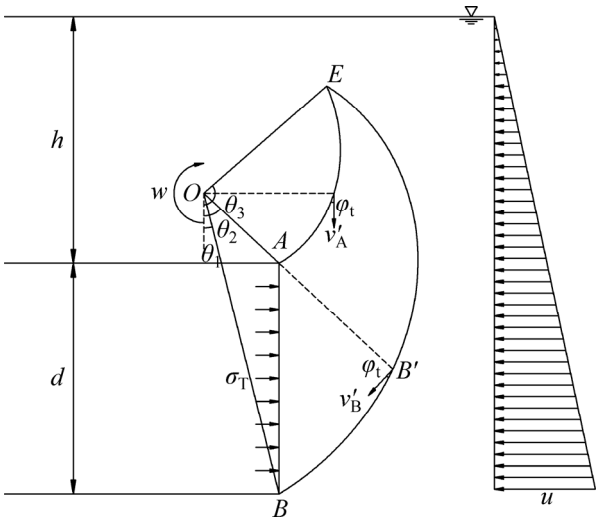

Fig. 2 Collapse mechanism of double-logarithmic spiral curves on face of deep tunnel [13]

The double-logarithmic curved collapse mechanism of tunnel faces in deep rock tunnels is simplified to a plane strain issue. According to the assumptions of upper bound theorem in limit analysis, the rock/soil masses follow the flow rule, thus the velocity at the random point in the logarithmic spiral curves has an angle of φ_t with the tangential line at this point, as shown in Fig. 2, and the equations for describing two logarithmic spiral lines AE, BE are as follows:

$$r_1(\theta) = r_a \exp[(\theta-\theta_2)\tan\varphi_t] \tag{10}$$

$$r_2(\theta) = r_b \exp[(\theta_1-\theta)\tan\varphi_t] \tag{11}$$

Due to the geometrical relationship in Fig. 2, r_a and r_b are the functions related to θ_1 and θ_2, while θ_3 is a function with regard of θ_1, θ_2 and φ_t, i.e.

$$r_a = \frac{\sin\theta_1}{\sin(\theta_2-\theta_1)}d \tag{12}$$

$$r_b = \frac{\sin\theta_2}{\sin(\theta_2-\theta_1)}d \tag{13}$$

$$\theta_3 = \frac{1}{2}[(\theta_1+\theta_2) - \frac{\ln(\sin\theta_1/\sin\theta_2)}{\tan\varphi_t}] \tag{14}$$

4 Computational process

4.1 Work rate of rock/soil mass

To easily calculate the work rate created by rock/soil weight, it is necessary to extend line OA to the line BE with an intersection B', thus the whole work rate of ABE can be expressed as $P_{\gamma 1}-P_{\gamma 2}+P_{\gamma 3}-P_{\gamma 4}$. Thereinto, $P_{\gamma 1}$, $P_{\gamma 2}$, $P_{\gamma 3}$, and $P_{\gamma 4}$ represent the power of gravity in the

regions *OB′E*, *OAE*, *OBB′* and *OAB*, respectively, and the specific expressions are shown as

$$P_{\gamma 1}=\int_{\theta_2}^{\theta_3}\frac{2}{3}\omega\cdot r_2(\theta)\cdot\sin\theta\cdot\frac{1}{2}\gamma\cdot r_2^2(\theta)\mathrm{d}\theta$$
$$=\gamma\cdot\omega\cdot r_b^3\cdot f_1(\theta_2,\theta_3) \tag{15}$$

where

$$f_1(\theta_2,\theta_3)=\frac{1}{3}\int_{\theta_2}^{\theta_3}\exp[3(\theta_1-\theta)\cdot\tan\varphi_t]\cdot\sin\theta\mathrm{d}\theta$$
$$=\{-\exp[3(\theta_1-\theta_3)\cdot\tan\varphi_t]\cdot(3\tan\varphi_t\cdot\sin\theta_3+\cos\theta_3)+\exp[3(\theta_1-\theta_2)\cdot\tan\varphi_t]\cdot(3\tan\varphi_t\cdot\sin\theta_2+\cos\theta_2)\}/[3(1+9\tan^2\varphi_t)] \tag{16}$$

$$P_{\gamma 2}=\int_{\theta_2}^{\theta_3}\frac{2}{3}\omega\cdot r_1(\theta)\cdot\sin\theta\cdot\frac{1}{2}\gamma\cdot r_1^2(\theta)\mathrm{d}\theta$$
$$=\gamma\cdot\omega\cdot r_a^3\cdot f_2(\theta_2,\theta_3) \tag{17}$$

$$f_2(\theta_2,\theta_3)=\frac{1}{3}\int_{\theta_2}^{\theta_3}\exp[3(\theta-\theta_2)\cdot\tan\varphi_t]\cdot\sin\theta\mathrm{d}\theta$$
$$=\{\exp[3(\theta_3-\theta_2)\cdot\tan\varphi_t]\cdot(3\tan\varphi_t\cdot\sin\theta_3-\cos\theta_3)+\cos\theta_2-3\tan\varphi_t\cdot\sin\theta_2\}/[3(1+9\tan^2\varphi_t)] \tag{18}$$

$$P_{\gamma 3}=\int_{\theta_1}^{\theta_2}\frac{2}{3}\omega\cdot r_2(\theta)\cdot\sin\theta\cdot\frac{1}{2}\gamma\cdot r_2^2(\theta)\mathrm{d}\theta$$
$$=\gamma\cdot\omega\cdot r_b^3\cdot f_3(\theta_1,\theta_2) \tag{19}$$

$$f_3(\theta_1,\theta_2)=\frac{1}{3}\int_{\theta_1}^{\theta_2}\exp[3(\theta_1-\theta)\cdot\tan\varphi_t]\cdot\sin\theta\mathrm{d}\theta$$
$$=\{-\exp[3(\theta_1-\theta_2)\cdot\tan\varphi_t]\cdot(3\tan\varphi_t\cdot\sin\theta_2+\cos\theta_2)+\cos\theta_1+3\tan\varphi_t\cdot\sin\theta_1\}/[3(1+9\tan^2\varphi_t)] \tag{20}$$

$$P_{\gamma 4}=\int_{\theta_1}^{\theta_2}\frac{1}{2}\cdot\frac{\sin\theta_1}{\sin\theta}\cdot r_b\cdot\frac{2}{3}\omega\cdot\frac{\sin^2\theta_1}{\sin^2\theta}\cdot r_b^2\cdot\sin\theta\mathrm{d}\theta$$
$$=\gamma\cdot\omega\cdot r_b^3\cdot f_4(\theta_1,\theta_2) \tag{21}$$

$$f_4(\theta_1,\theta_2)=\frac{1}{3}\int_{\theta_1}^{\theta_2}\frac{\sin^3\theta_1}{\sin^2\theta}\mathrm{d}\theta=\frac{1}{3}\sin^3\theta_1\cdot\left(\frac{\cos\theta_1}{\sin\theta_1}-\frac{\cos\theta_2}{\sin\theta_2}\right) \tag{22}$$

To sum up, the total power produced by mass in the region *ABE* is

$$P_\gamma=P_{\gamma 1}-P_{\gamma 2}+P_{\gamma 3}-P_{\gamma 4}$$
$$=\gamma\cdot\omega\cdot r_b^3\cdot(f_1+f_3-f_4)-\gamma\cdot\omega\cdot r_a^3\cdot f_2 \tag{23}$$

4.2 Power of pore water pressure

The rock/soil masses in failure are regarded as the rigid block which indicates that the volume is a constant, i.e. $\dot{\varepsilon}_{ij}=0$, thus the power of pore water pressure is sorely generated at the boundary. The work rates of pore water pressure at the boundaries *AE* and *BE*, i.e. P_{u1} and P_{u2}, can be written as

$$P_{u1}=\int_{\theta_2}^{\theta_3}r_u\cdot\gamma\cdot r_1^2(\theta)\cdot\omega\cdot\sin\varphi_t\cdot[r_1(\theta)\cos\theta+h-r_a\cos\theta_2]\mathrm{d}\theta$$
$$=r_u\cdot\gamma\cdot r_a^3\cdot\omega\cdot\sin\varphi_t\cdot f_5(\theta_2,\theta_3)+r_u\cdot\gamma\cdot r_a^2\cdot\omega\cdot\sin\varphi_t\cdot(h-r_a\cos\theta_2)\cdot f_6(\theta_2,\theta_3) \tag{24}$$

where

$$f_5(\theta_2,\theta_3)=\int_{\theta_2}^{\theta_3}\exp[3(\theta-\theta_2)\cdot\tan\varphi_t]\cdot\cos\theta\mathrm{d}\theta$$
$$=\{\exp[3(\theta_3-\theta_2)\cdot\tan\varphi_t]\cdot(\sin\theta_3+3\tan\varphi_t\cdot\cos\theta_3)-\sin\theta_2-3\tan\varphi_t\cdot\cos\theta_2\}/(1+9\tan^2\varphi_t) \tag{25}$$

$$f_6(\theta_2,\theta_3)=\int_{\theta_2}^{\theta_3}\exp[2(\theta-\theta_2)\cdot\tan\varphi_t]\mathrm{d}\theta$$
$$=\{\exp[2(\theta_3-\theta_2)\cdot\tan\varphi_t]-1\}/(2\tan\varphi_t) \tag{26}$$

$$P_{u2}=\int_{\theta_1}^{\theta_3}r_u\cdot\gamma\cdot r_2^2(\theta)\cdot\omega\cdot\sin\varphi_t\cdot[r_2(\theta)\cos\theta+h+d-r_b\cos\theta_1]\mathrm{d}\theta$$
$$=r_u\cdot\gamma\cdot r_b^3\cdot\omega\cdot\sin\varphi_t\cdot f_7(\theta_1,\theta_3)+r_u\cdot\gamma\cdot r_b^2\cdot\omega\cdot\sin\varphi_t\cdot(h+d-r_b\cos\theta_1)\cdot f_8(\theta_1,\theta_3) \tag{27}$$

$$f_7(\theta_1,\theta_3)=\int_{\theta_1}^{\theta_3}\exp[3(\theta_1-\theta)\cdot\tan\varphi_t]\cdot\cos\theta\mathrm{d}\theta$$
$$=\{\exp[3(\theta_1-\theta_3)\cdot\tan\varphi_t]\cdot(\sin\theta_3-3\tan\varphi_t\cdot\cos\theta_3)-\sin\theta_1+3\tan\varphi_t\cdot\cos\theta_1\}/(1+9\tan^2\varphi_t) \tag{28}$$

$$f_8(\theta_1,\theta_3)=\int_{\theta_1}^{\theta_3}\exp[2(\theta_1-\theta)\cdot\tan\varphi_t]\mathrm{d}\theta$$
$$=\{1-\exp[2(\theta_1-\theta_3)\cdot\tan\varphi_t]\}/(2\tan\varphi_t) \tag{29}$$

Consequently, the whole power of pore water pressure results in

$$P_u=P_{u1}+P_{u2}=r_u\cdot\gamma\cdot r_a^2\cdot\omega\cdot\sin\varphi_t\cdot[r_a\cdot f_5+(h-r_a\cos\theta_2)\cdot f_6]+r_u\cdot\gamma\cdot r_b^2\cdot\omega\cdot\sin\varphi_t\cdot[r_b\cdot f_7+(h+d-r_b\cos\theta_1)\cdot f_8] \tag{30}$$

4.3 Work rate of supporting pressure

Concerning the collapse pressure applied on the faces of deep rock tunnels, i.e. the required supporting pressure for guaranteeing the stability of tunnel faces, it can be regarded as uniform load with simplification, σ_T, thus the corresponding power can be worked out based on upper bound theorem.

$$P_T=\int_{\theta_1}^{\theta_2}\frac{r_b}{\sin\theta}\cdot\sin\theta_1\cdot\omega\cdot\cos\theta\cdot\sigma_T\cdot\frac{r_b}{\sin^2\theta}\cdot\sin\theta_1\mathrm{d}\theta$$
$$=\frac{1}{2}\sigma_T\cdot\omega\cdot r_b^2\cdot\left(1-\frac{\sin^2\theta_1}{\sin^2\theta_2}\right) \tag{31}$$

4.4 Internal energy dissipation

As to rigid block *ABE* with $\dot{\varepsilon}_{ij}=0$, the internal energy would just dissipate along the velocity discontinuity lines *EA* and *EB*, thus the total internal energy dissipation P_V can be calculated, and P_{V1} and P_{V2}

respectively represent the energy dissipation on *EA* and *EB*, i.e.

$$P_V = P_{V1} + P_{V2} = \int_{\theta_2}^{\theta_3} r_1(\theta)\cdot\omega\cdot\cos\varphi_t\cdot c_t\cdot r_1(\theta)\mathrm{d}\theta + \int_{\theta_1}^{\theta_3} r_2(\theta)\cdot\omega\cdot\cos\varphi_t\cdot c_t\cdot r_2(\theta)\mathrm{d}\theta = c_t\cdot\omega\cdot\cos^2\varphi_t\cdot\{r_a^2\cdot(\exp[2(\theta_3-\theta_2)\cdot\tan\varphi_t]-1)+ r_b^2\cdot(1-\exp[2(\theta_1-\theta_3)\cdot\tan\varphi_t])\}/(2\sin\varphi_t) \quad (32)$$

4.5 Upper bound solutions of supporting pressure

According to the virtual power principle of limit analysis, the collapse pressure of tunnel faces can be derived by equating the external work rate to the internal energy dissipation, thus the analytic solution of supporting pressure (collapse pressure) can be expressed through simultaneous calculation of Eqs. (23), (30)−(32).

$$\sigma_T = \frac{2(P_\gamma + P_u - P_V)}{\omega\cdot r_b^2\cdot(1-\dfrac{\sin^2\theta_1}{\sin^2\theta_2})} \quad (33)$$

Moreover, the parameters in Eq. (33) should satisfy the following constraints as

$$\begin{cases} 0<\theta_1<\theta_2<\pi/2 \\ \theta_2<\theta_3<\pi \\ r_a<r_b \end{cases} \quad (34)$$

To guarantee the stability of tunnel faces, the maximal magnitude of collapse pressure should be calculated. It can be easily found from Eq. (33) that the collapse pressure (supporting pressure), σ_T, is a function related to θ_1, θ_2 and φ_t, i.e. $\sigma_T = f(\theta_1,\theta_2,\varphi_t)$. Therefore, the problem of calculating the maximal value of collapse pressure is converted to a mathematical optimization model, i.e. searching the maximal value of the objective function, $\sigma_T = f(\theta_1,\theta_2,\varphi_t)$, under the constraints in Eq. (34), which is the most optimal upper bound solution of collapse pressure and is also the minimal supporting pressure for maintaining the stability of tunnel faces. The upper bound solutions can be calculated with MATLAB software programming and sequence quadratic iterative algorithm, and the detail optimization process is not introduced here.

5 Analysis of results

5.1 Comparison

Based on limit analysis method, SENENT et al [32] obtained the upper bound solution of collapse pressure with nonlinear Hoek-Brown failure criterion when they investigated the face stability of shallow rock tunnels. To verify the correctness of the method in this work, the introduced collapse pressure ratio of tunnel faces in deep stratum gained from this work, $\sigma_T/(\gamma d)$, is compared with that derived from shallow tunnels by SENENT et al [32], as shown in Fig. 3. In the process of comparison, the parameters should be the same with those in Ref. [32], i.e., soil weight γ=25 kN/m^3, tunnel diameter d=10 m, rock constant m_i=5, disturbance factor D=0. It can be seen from Fig. 3 that, with the increase of uniaxial compressive strength ratio, $\sigma_{ci}/(\gamma d)$, the change law of $\sigma_T/(\gamma d)$ calculated from this work is consistent with that refereed to Ref. [32] when geological strength parameters are I_{GS}=10 and I_{GS}=15, which shows the validity of proposed approach in this work.

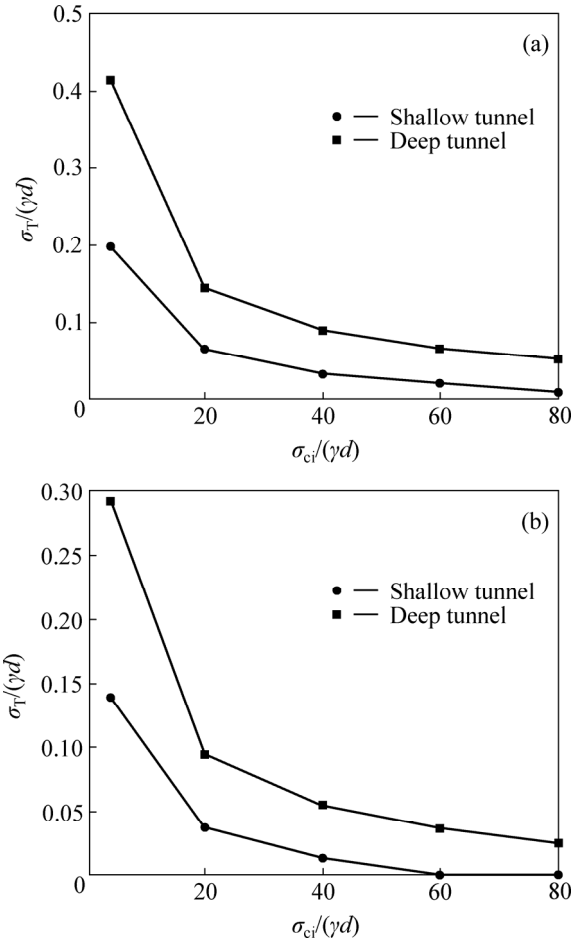

Fig. 3 Influence of ratio of uniaxial compressive strength on ratio of collapse pressure: (a) I_{GS}=10; (b) I_{GS}=15

5.2 Effect of nonlinear Hoek-Brown failure criterion on face stability

Due to great disturbance or weak surrounding rock, the tunnel faces would collapse under excavations in deep rock layers, thus the influence of nonlinear Hoek-Brown failure criterion on collapse pressure and failure surface of tunnel faces is greatly investigated apart from the research of pore water pressure, as shown in Figs. 4−9. Parameters are: soil weight per volume γ= 25 kN/m^3, tunnel diameter d=10 m, the coefficient of pore water pressure r_u=0.3, and the height between underground waterline and tunnel roof h=30 m.

The influence of I_{GS} and m_i on collapse pressure of tunnel faces is shown in Fig. 4 when the corresponding parameters are $\sigma_{ci}=600$ kPa and D=0.5. It can be found from Fig. 4 that with the increase of I_{GS} and m_i, the collapse pressure would decrease. When I_{GS}=20 and m_i=15, the influence of σ_{ci} and D on collapse pressure of tunnel faces is illustrated in Fig. 5 from which one can notice that with the increasing value of σ_{ci}, the collapse pressure tends to decrease, while it has a

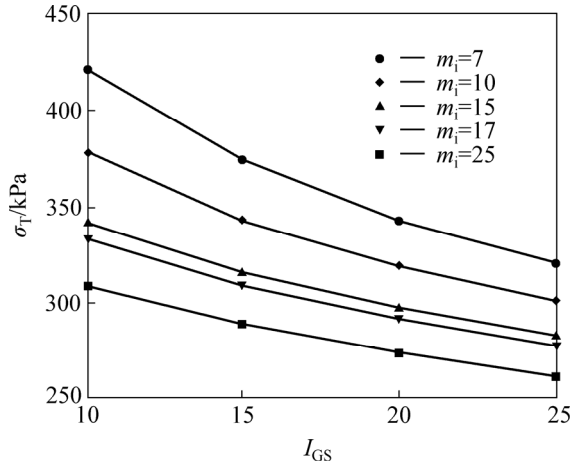

Fig. 4 Influences of I_{GS} and m_i on collapse pressure

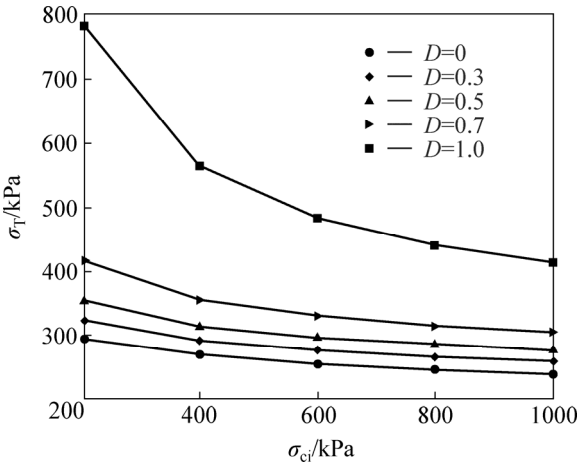

Fig. 5 Influence of σ_{ci} and D on collapse pressure

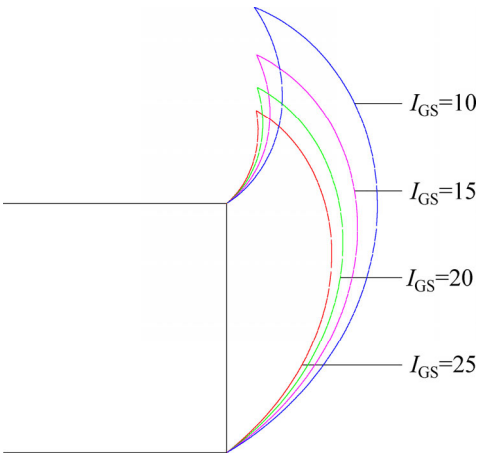

Fig. 6 Influence of I_{GS} on collapse shape

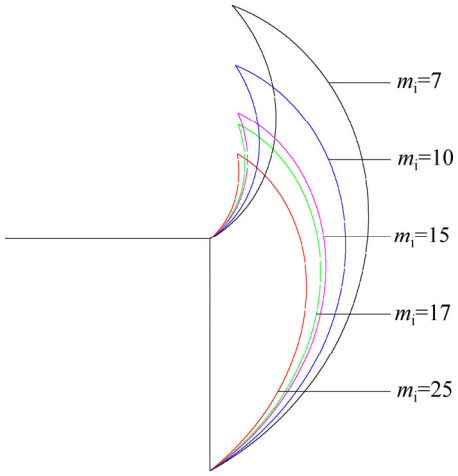

Fig. 7 Influence of m_i on collapse shape

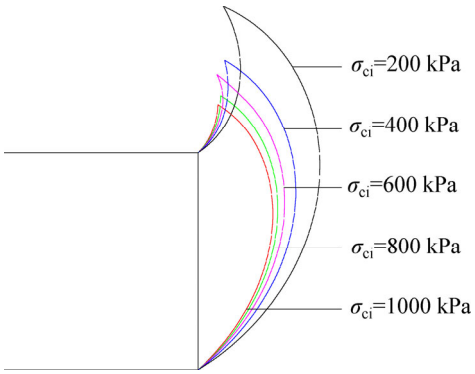

Fig. 8 Influence of σ_{ci} on collapse shape

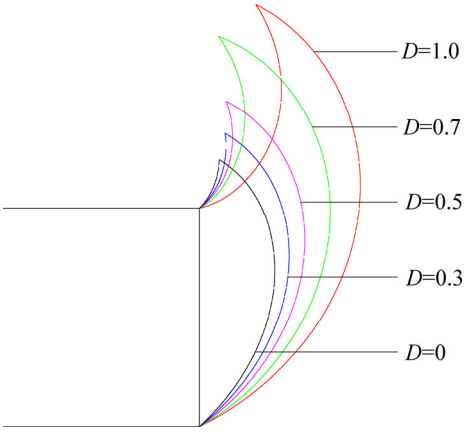

Fig. 9 Influence of D on collapse shape

tendency to increase with the increase of D. In conclusion, nonlinear Hoek-Brown failure criterion has a large impact on the collapse pressure of face in deep rock tunnels.

The effect of I_{GS} on failure shape is shown in Fig. 6 with m_i=25, $\sigma_{ci}=600$ kPa and D=0.5. In Fig. 6, the collapse area of tunnel faces in deep-buried rock tunnels tends to decrease since the greater the I_{GS}, the better the quality of surrounding rock masses and the less the failure region of tunnel faces. When I_{GS}=25, $\sigma_{ci}=600$ kPa and D=0.5, the influence of m_i on

collapse shape is illustrated in Fig. 7 from which it can be noticed that the bigger value of m_i would induce smaller failure region because the greater magnitude of m_i means better surrounding rock which could reduce the collapse area. The effect of σ_{ci} on failure shape is shown in Fig. 8 with I_{GS}=20, m_i=15 and D=0. The change rule and interpretation of collapse region with regard of σ_{ci} is similar to that with I_{GS} and m_i. Meanwhile, the impact of D on collapse area is shown in Fig. 9 with I_{GS}=20, m_i=15 and σ_{ci} = 1000 kPa . It can be seen from Fig. 9 that with the increase of D, the corresponding failure surface tends to increase since the larger value of D means greater disturbance of surrounding rock, which leads to the bigger collapse region. Consequently, nonlinear Hoek-Brown failure criterion has a greater influence on the collapse scope of tunnel faces in deep-buried rock tunnels.

5.3 Impact of pore water pressure on face stability

When tunnels are under excavations in deep rock masses, an important factor, the effect of water, contributes to the collapse of tunnel faces. In this case, on the basis of nonlinear Hoek-Brown failure criterion, more attention is paid to the impact of pore water pressure on collapse pressure and failure shape of tunnel faces in deep rock tunnels, as shown in Figs. 10−12. The corresponding parameters are: soil weight γ=25 kN/m^3, tunnel diameter d=10 m, geological strength index I_{GS}=20, uniaxial compressive strength σ_{ci} = 600 kPa and disturbance factor D=0.5.

The influence of pore water pressure coefficient, r_u and waterline height, h, on the collapse pressure of tunnel faces is shown in Fig. 10 from which it can be found that with the increasing value of r_u or h, the corresponding collapse pressure would increase significantly, which illustrates that pore water pressure has an important effect on the collapse pressure of tunnel faces in deep-buried stratum.

When the height between underground waterline and the tunnel roof h=10 m, the influence of pore water pressure coefficient, r_u, on failure shape of tunnel faces is shown in Fig. 11. It is manifest from Fig. 11 that the greater magnitude of r_u would induce larger collapse region, which means that abundant pore water produces greater pore water pressure which leads to larger failure scope. Similarly, the impact of h on collapse shape of tunnel faces is illustrated in Fig. 12 with r_u=0.5 from which one can find that the larger value of h and the greater failure area occurring in front of tunnel faces. Consequently, the collapse shape and region of tunnel faces are greatly influenced by pore water in deep rock tunnels.

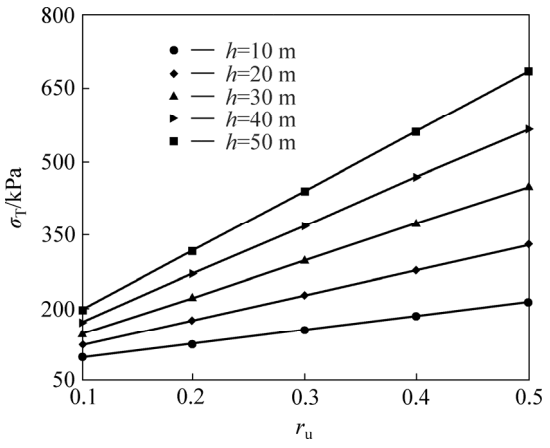

Fig. 10 Influences of r_u and h on collapse pressure

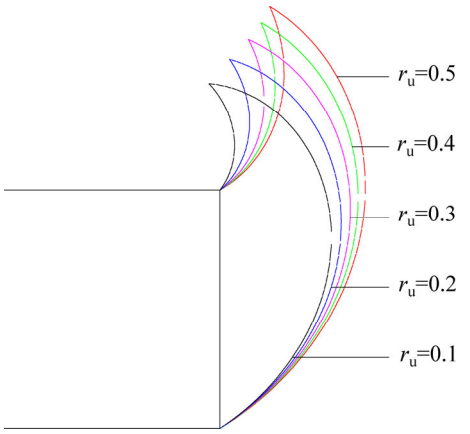

Fig.11 Influence of r_u on collapse shape

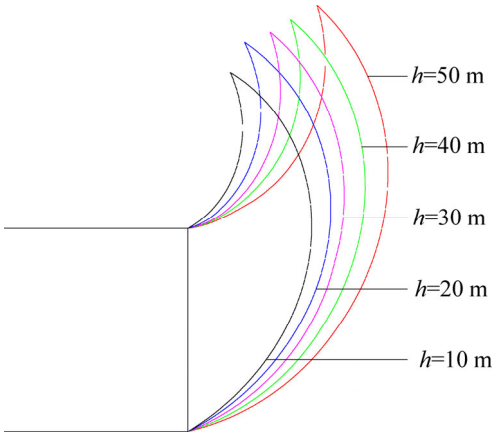

Fig.12 Influence of h on collapse shape

6 Conclusions

1) Based on nonlinear Hoek-Brown failure criterion, the analytic solutions of collapse pressure of tunnel faces in deep rock stratum are deduced with upper bound theorem when considering the effect of pore water, and the most optimal upper bound solution is derived through optimization programme.

2) The collapse pressure ratio of face of deep tunnels calculated is compared with that gained in shallow tunnels with the same parameters, and the consistency of changing law verified the validity of the proposed approach.

3) Nonlinear Hoek-Brown failure criterion for describing the rock characteristics has a great influence on the collapse pressure and failure shape of face in deep rock tunnels. Specifically, with the increase of I_{GS}, m_i and σ_{ci}, the collapse pressure and the collapse scope would tend to decrease, while the collapse pressure and failure region are positive to the value of D. In the practical projects, the effect of pore water pressure on face stability should be not ignorable since the greater magnitude of r_u or h would induce larger collapse pressure and failure scope significantly. Therefore, as to deep rock tunnels, when there exists poor surrounding rock, great disturbance or rich pore water, the supporting measures should be strengthened and timely monitoring measurement should also be conducted so as to prevent the occurrence of face collapse.

References

[1] YANG Xiao-li, YANG zi-han, PAN Qiu-jing, LI Yu-lin. Kinematical analysis of highway tunnel collapse using nonlinear failure criterion [J]. Journal of Central South University, 2014, 21(1): 381−386.

[2] SAADA Z, MAGHOUS S, GARNIER D. Pseudo-static analysis of tunnel face stability using the generalized Hoek-Brown strength criterion [J]. International Journal for Numerical and Analytical Methods in Geomechanics, 2013, 37(18): 3194−3212.

[3] YANG X L, WANG J M. Ground movement prediction for tunnels using simplified procedure [J]. Tunnelling and Underground Space Technology, 2011, 26(3): 462−471.

[4] FRALDI M, GUARRACINO F. Analytical solutions for collapse mechanisms in tunnels with arbitrary cross sections [J]. International Journal of Solids and Structures, 2010, 47(2): 216−223.

[5] YANG Xiao-li, JIN Qi-yun, MA Jun-qiu. Pressure from surrounding rock of three shallow tunnels with large section and small spacing [J]. Journal of Central South University, 2012, 19(8): 2380−2385.

[6] LECA E, DORMIEUX L. Upper and lower bound solutions for the face stability of shallow circular tunnels in frictional material [J]. Géotechnique, 1990, 40(4): 581−606.

[7] SOUBRA A H. Three-dimensional face stability analysis of shallow circular tunnels [C]// International Conference on Geotechnical and Geological Engineering. Melbourne, Australia: ICGGE, 2000: 19−24.

[8] MOLLON G, PHOON K K, DIAS D, SOUBRA A H. Validation of a new 2D failure mechanism for the stability analysis of a pressurized tunnel face in a spatially varying sand [J]. Journal of Engineering Mechanics, 2010, 137(1): 8−21.

[9] YANG Xiao-li, ZHANG Dao-bing, WANG Zuo-wei. Upper bound solutions for supporting pressures of shallow tunnels with nonlinear failure criterion [J]. Journal of Central South University, 2013, 20(7): 2034−2040.

[10] YANG X L, HUANG F. Three-dimensional failure mechanism of a rectangular cavity in a Hoek-Brown rock medium [J]. International Journal of Rock Mechanics and Mining Sciences, 2013, 61: 189−195.

[11] MOLLON G, DIAS D, SOUBRA A H. Rotational failure mechanisms for the face stability analysis of tunnels driven by a pressurized shield [J]. International Journal for Numerical and Analytical Methods in Geomechanics, 2011, 35(12): 1363−1388.

[12] MOLLON G, DIAS D, SOUBRA A H. Range of the safe retaining pressures of a pressurized tunnel face by a probabilistic approach [J]. Journal of Geotechnical and Geoenvironmental Engineering, 2013, 139(11): 1954−1967.

[13] SUBRIN D, WONG H. Tunnel face stability in frictional material: A new 3D failure mechanism [J]. Comptes Rendus Mecanique, 2002, 330(7): 513−519.

[14] HOEK E, CARRANZE-TORRES C, CORKUM B. Hoek-Brown failure criterion-2002 edition [C]//Proceedings of the North American Rock Mechanics Society Meeting. Toronto, 2002: 267−273.

[15] YANG X L, QIN C B. Limit analysis of rectangular cavity subjected to seepage forces based on Hoek-Brown failure criterion [J]. Geomechanics and Engineering, 2014, 6(5): 503−515.

[16] YANG X L, YIN J H. Upper bound solution for ultimate bearing capacity with a modified Hoek-Brown failure criterion [J]. International Journal of Rock Mechanics and Mining Sciences, 2005, 42(4): 550−560.

[17] YANG X L, HUANG F. Collapse mechanism of shallow tunnel based on nonlinear Hoek-Brown failure criterion [J]. Tunnelling and Underground Space Technology, 2011, 26(6): 686−691.

[18] LI A J, MERIFIELD R S, LYAMIN A V. Effect of rock mass disturbance on the stability of rock slopes using the Hoek-Brown failure criterion [J]. Computers and Geotechnics, 2011, 38(4): 546−558.

[19] YANG X L, YIN J H. Slope stability analysis with nonlinear failure criterion [J]. Journal of Engineering Mechanics, 2004, 130(3): 267−273.

[20] YANG X L. Seismic passive pressures of earth structures by nonlinear optimization [J]. Archive of Applied Mechanics, 2011, 81(9): 1195−1202.

[21] YANG X L, YIN J H. Slope equivalent Mohr-Coulomb strength parameters for rock masses satisfying the Hoek-Brown criterion [J]. Rock Mechanics and Rock Engineering, 2010, 43(4): 505−511.

[22] MAO N, AL-BITTAR T, SOUBRA A H. Probabilistic analysis and design of strip foundations resting on rocks obeying Hoek-Brown failure criterion [J]. International Journal of Rock Mechanics and Mining Sciences, 2012, 49: 45−58.

[23] VIRATJANDR C, MICHALOWSKI R L. Limit analysis of submerged slopes subjected to water drawdown [J]. Canadian Geotechnical Journal, 2006, 43(8): 802−814.

[24] SHIN H S, YOUN D J, CHAE S E, SHIN J H. Effective control of pore water pressures on tunnel linings using pin-hole drain method [J]. Tunneling and Underground Space Technology, 2009, 24(5): 555−561.

[25] MICHALOWSKI R L, NADUKURU S S. Three-dimensional limit analysis of slopes with pore pressure [J]. Journal of Geotechnical and Geoenvironmental Engineering, 2012, 139(9): 1604−1610.

[26] SHIN J H. Analytical and combined numerical methods evaluating pore water pressure on tunnels [J]. Géotechnique, 2010, 60(2): 141−145.

[27] CHEN W F. Limit analysis and soil plasticity [M]. Florida: J. Ross Publishing, Inc., 2007: 47−99.

[28] YANG X L, ZOU J F. Cavity expansion analysis with non-linear failure criterion [J]. Proceedings of the Institution of Civil Engineers-Geotechnical Engineering, 2011, 164(1): 41−49.

[29] GEREMEW A M. Pore-water pressure development caused by wave-induced cyclic loading in deep porous formation [J]. International Journal of Geomechanics, 2011, 13(1): 65−68.

[30] YANG X L. Seismic bearing capacity of a strip footing on rock slopes [J]. Canadian Geotechnical Journal, 2009, 46(8): 943−954.

[31] YANG Xiao-li, SUI Zhi-rong. Seismic failure mechanisms for loaded slopes with associated and nonassociated flow rules [J]. Journal of Central South University of Technology, 2008, 15(2): 276−279.

[32] SENENT S, MOLLON G, JIMENEZ R. Tunnel face stability in heavily fractured rock masses that follow the Hoek-Brown failure criterion [J]. International Journal of Rock Mechanics and Mining Sciences, 2013, 60(1): 440−451.

(Edited by DENG Lü-xiang)